Floquet Engineering Correlated Materials with Unpolarized Light

V. L. Quito* and R. Flint
Department of Physics and Astronomy, Iowa State University, Ames, Iowa 50011, USA

(Received 26 March 2020; accepted 2 March 2021; published 27 April 2021)

Floquet engineering is a powerful tool that drives materials with periodic light. Traditionally, the light is monochromatic, with amplitude, frequency, and polarization varied. We introduce Floquet engineering via unpolarized light built from quasimonochromatic light and show how it can modify strongly correlated systems, while preserving the original symmetries. Different types of unpolarized light can realize different strongly correlated phases As an example, we treat insulating magnetic materials on a triangular lattice and show how unpolarized light can induce a Dirac spin liquid.

DOI: 10.1103/PhysRevLett.126.177201

Floquet engineering provides a powerful method to access and control phases and phenomena absent or rare in equilibrium [1–10]. In its most common application, Floquet engineering consists of continuously driving a sample with monochromatic laser light, which has a fixed polarization. Unless the polarization axis is preserved by lattice symmetries, polarized light explicitly breaks either lattice (linear polarization), time-reversal (circular polarization), or both symmetries. This explicit symmetry breaking can be useful, as new couplings like chiral fields that induce spin chirality [11–14] or anomalous Hall effects [15–17] can be generated; or spatial anisotropies and dimensionalities can be tuned [18–22]. While polarized light drives interesting physics [1,23,24], some correlated phases are only accessible if all symmetries are preserved. For example, symmetric spin liquids require preserving lattice and time-reversal symmetries [25]. These phases are found in equilibrium models, but are confined to small regions of phase space theoretically and are extremely rare experimentally. Floquet engineering could provide a new way to access spin liquids in materials and to tune across their quantum critical points.

Unpolarized light preserves symmetries, but is not strictly monochromatic. Thus, it is not obvious that Floquet techniques apply or what the effect is on correlated materials, although some promising work analyzed the effect of noise in Floquet engineered graphene [26]. This Letter provides the general theory and applicability of unpolarized light in Floquet systems. Different kinds of unpolarized light sample polarizations differently, understood as different paths over the Poincaré sphere shown in Fig. 1. We prove that Floquet engineering with effectively unpolarized light is possible and introduce a simple model with two oppositely circularly polarized lasers whose frequencies are slightly detuned, resulting in unpolarized light whose polarization vector explores the equator of the Poincaré sphere. We calculate the effect on magnetic exchange interactions in Mott insulators and show that polarization averaging of the final result agrees with the exact result for sufficiently slow variation of the polarization vector. We then consider all types of unpolarized light and show how varied realistic choices can give significantly different exchange couplings while preserving the same symmetries. We treat the half filled triangular Hubbard model in detail and show how to boost the ratio of J_2/J_1 and potentially access both the Dirac [27–34] spin liquid

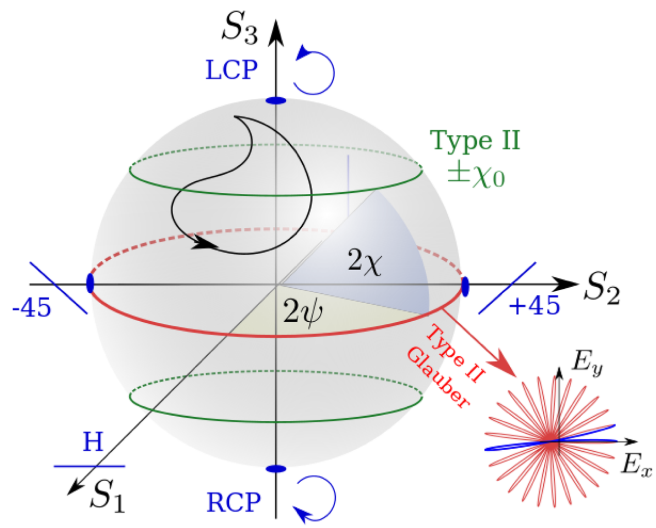

FIG. 1. The Poincaré sphere captures all polarization profiles. The axes are the Stokes parameters, which give the degree of horizontal and vertical (S_1), ±45° (S_2), and circular (S_3) polarization. The monochromatic light traditionally used in Floquet engineering corresponds to a single point. Unpolarized light corresponds to *paths* on the sphere with $\langle \vec{S} \rangle = 0$. As we show, different paths can lead to distinct correlated phases. Any parallel of constant latitude χ preserves rotational symmetry (e.g., red curve). If parallels of both $\pm\chi$ are included (green curves), time reversal is also preserved. Inset: parametric plot of the electric field of our simple example, where the polarization traverses the equator with period T_p. The thick blue line shows a single period T.

and the time-reversal symmetry breaking chiral spin liquid [32,33,35,36]. Finally, we discuss how Floquet engineering with unpolarized light may be reasonably implemented experimentally.

We examine magnetic exchange couplings in a single-band Floquet-Hubbard model, where electrons hop on a lattice in the presence of a time-dependent electric field, $\boldsymbol{E} = -\frac{\partial \boldsymbol{A}}{\partial t}$. There is a strong penalty for double occupancy U,

$$\mathcal{H}_0 = -t_1 \sum_{i,\boldsymbol{\delta}_i} e^{-i\boldsymbol{A}(t)\cdot\boldsymbol{\delta}_i} c_i^\dagger c_{i+\boldsymbol{\delta}_i} + U \sum_i n_{i\uparrow} n_{i\downarrow} - \mu \sum_i n_i. \quad (1)$$

The chemical potential μ is adjusted to ensure half filling. We consider only nearest-neighbor links labeled by $\boldsymbol{\delta}_i = (\cos\phi_i, \sin\phi_i)$ and assume light propagation normal to the sample. We take the vector potential to be time periodic, with period $T = 2\pi/\Omega$, which allows the Fourier transform to Floquet space with the *discrete* set of frequencies [37–40] $m\Omega$, $m \in \mathbb{Z}$. In this space, the electrons now hop not just between sites, but between Floquet sectors labeled by $|m\rangle$ [1,40],

$$\begin{aligned}\mathcal{H} = &-\sum_{m,n} \sum_{i,\boldsymbol{\delta}_i} t_{i,i+\boldsymbol{\delta}_i}^{(n-m)} c_i^\dagger c_{i+\boldsymbol{\delta}_i} |m\rangle\langle n| \\ &+ \sum_m \sum_i (U n_{i\uparrow} n_{i\downarrow} + m\Omega) |m\rangle\langle m|. \end{aligned} \quad (2)$$

One key feature is that Ω may be tuned such that $m\Omega = -U$ for some integer m. If so, pairs of doublons and holons will be excited across the Hubbard gap [41–46], a resonance that destroys the Mott insulating state. However, for frequencies away from these resonances, which have width $\sim t_1$, the heating is minimal and an effective spin model treatment is justified [14].

Typically, the Floquet formalism treats a single frequency Ω, but we now extend it to quasimonochromatic unpolarized light. We consider light combining two circularly polarized beams with slight frequency detuning, which causes the polarization vector to circle the equator, as shown in the inset of Fig. 1, sampling all linear polarizations equally. We call the two frequencies $\Omega_\pm \equiv \Omega \pm \Omega_p$ and require that they be commensurate to ensure overall time periodicity. We assume that the period of the light $T = 2\pi/\Omega$ is small compared to the period of the polarization $T_p = 2\pi/\Omega_p$, and the commensurability is ensured by taking $T_p = NT$, where N is an integer that is large for quasimonochromatic light. The electric field is

$$\begin{aligned}\boldsymbol{E}(t) &= E_0 \begin{pmatrix} \cos\Omega_p t \\ \sin\Omega_p t \end{pmatrix} \mathrm{Re}(e^{-i\Omega t}), \\ &= \frac{E_0}{2} \mathrm{Re}\left[\begin{pmatrix} 1 \\ i \end{pmatrix} e^{-i\Omega_+ t} + \begin{pmatrix} 1 \\ -i \end{pmatrix} e^{-i\Omega_- t} \right]. \end{aligned} \quad (3)$$

We can use perturbation theory to find the magnetic exchange couplings numerically for any integer N and analytically for large but finite N; exactly at $N = \infty$, the light is linearly polarized. We first find the effective hoppings between sites and Floquet sectors, generically given by $t_{i,i+\boldsymbol{\delta}_i}^{(m)} = t_1/(2\pi) \int_0^{2\pi} d\theta e^{-im\theta} e^{i\boldsymbol{A}(\theta)\cdot\boldsymbol{\delta}}$ [1], where $\theta = \Omega_p t$ and $\boldsymbol{A}(t) = -\int^t dt' \boldsymbol{E}(t')$. In our particular case,

$$t_{i,i+\boldsymbol{\delta}_i}^{(m)} = \frac{t_1}{2\pi} \int_0^{2\pi} d\theta e^{-im\theta} e^{iA_+ \sin\tilde{\theta}_+ + iA_- \sin\tilde{\theta}_-}, \quad (4)$$

where $A_\pm = A_0(1 \pm N^{-1})^{-1}$, with fluence $A_0 = E_0/(2\Omega)$, and $\tilde{\theta}_\pm = \theta(N \pm 1) \mp \phi_i$, where ϕ_i gives the directional dependence. The integral can be performed by decomposing both ($\pm$) exponentials into sums over Bessel functions using $\exp(ix \sin\rho) = \sum_{m'} \mathcal{J}_{m'}(x) e^{im'\rho}$ [47],

$$\begin{aligned} t_{i,i+\boldsymbol{\delta}_i}^{(m)} = t_1 &\sum_{m_1,m_2=-\infty}^{+\infty} \mathcal{J}_{m_1}(A_+) \mathcal{J}_{m_2}(A_-) e^{-i(m_1-m_2)\phi_l} \\ &\times \delta_{m-N(m_1+m_2)+m_2-m_1}. \end{aligned} \quad (5)$$

The sums over $m_{1,2}$ can be calculated numerically for any integer N. It is convenient to parametrize $m = N\tilde{m} + k$, with $\tilde{m} = m_1 + m_2$ and $k = m_2 - m_1$ integers, which allows the hopping to be written as $t_{i,i+\boldsymbol{\delta}_l}^{(N\tilde{m}+k)} \equiv t_1 f_k^{\tilde{m}} e^{-ik\phi_l}$, with $f_k^{\tilde{m}} = \mathcal{J}_{\frac{1}{2}(\tilde{m}+k)}(A_+) \mathcal{J}_{\frac{1}{2}(\tilde{m}-k)}(A_-)$. For sufficiently large N, the non-negligible amplitudes $f_k^{\tilde{m}}$ are tightly clustered around each $\tilde{m}$, with $k \approx 0$. An example hopping profile is shown in Fig. 2(a) as function of m. We can now calculate the nearest-neighbor exchange couplings for each direction $J_1^{(\boldsymbol{\delta}_l)}$ expanding in the excited energies, $U + (N\tilde{m} + k)\Omega_p$ [48–50],

$$J_1^{(\boldsymbol{\delta}_l)} = 4 \sum_{\tilde{m},k} \frac{t_l^{(N\tilde{m}+k)} t_l^{(-N\tilde{m}-k)}}{U + (N\tilde{m} + k)\Omega_p}. \quad (6)$$

The results as a function of fluence A_0 are shown in Fig. 2(b) for fixed frequency and several values of N. For small N, J_1 is direction dependent (results are for $\boldsymbol{\delta}_1$ on the triangular lattice, with $\phi_1 = \pi/3$). As N increases, J_1 becomes isotropic and converges to the average over linearly polarized monochromatic light.

We now discuss the limit of large but finite N, where we obtain analytical results. We note that the hoppings, Eq. (5), are dominated by contributions from $m \approx N\tilde{m}$, allowing the sums to be truncated for $k \ll N$. For large N, $A_+ \approx A_- \approx A_0$. As the numerators of Eq. (6) are dominated by small k/N for each $\tilde{m}$, we approximate

$$J_1^{(\boldsymbol{\delta}_l)} \approx 4t_1^2 \sum_{\tilde{m}} \frac{\sum_k |f_k^{\tilde{m}}|^2}{U + \tilde{m}\Omega}. \quad (7)$$

Here, we neglect the k dependence of the denominator, but one must be careful, as the k dependence appears to give

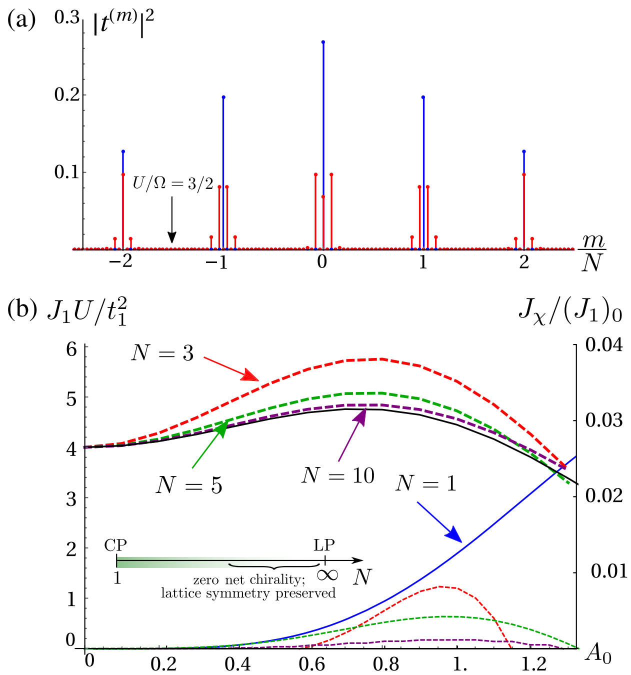

FIG. 2. (a) The hopping terms $|t^{(m)}|^2$ (red) as a function of m, for $N = 25$ and $A_0 = 1.5$. The non-negligible values cluster around $m = N\tilde{m}$ with small satellite peaks. When these clusters are well separated, as for sufficiently large N, the contribution of each cluster can be summed to give an approximate $|t^{(\tilde{m})}|^2$ (blue). It is important to avoid resonances with non-negligible weight. The arrow indicates our chosen frequency with $m/N = -3/2$ for $N\Omega_p/U = \Omega/U = 2/3$, where the amplitude of $|t^{(m)}|^2$ is vanishingly small. (b) J_1 as a function of fluence A_0. The black line indicates the monochromatic average over LPs, which coincides with the $N \geq 25$ results. Also shown with dashed lines are chiral couplings on a triangular lattice J_χ, normalized by the bare $(J_1)_0$. $N = 1$ corresponds to the circularly polarized case. As N increases, J_χ becomes vanishingly small.

further resonances at *every* k value. The numerators are strongly suppressed in k/N, however, as shown in Fig. 2(a), and so only the resonances near the main $\Omega = -U/\tilde{m}$ resonance are dangerous. The above result then takes the same form as the magnetic exchange couplings for monochromatic light with *effective* hoppings $t_1\sqrt{\sum_k |f_k^{\tilde{m}}|^2}$. These are independent of ϕ_l, making $J_1^{(\delta_l)}$ isotropic, and $f_k^{\tilde{m}}$ is even with respect to k, which guarantees that chiral terms vanish for large N [51]. Chiral fields (J_χ) couple to the scalar chirality $\vec{S}_i \cdot (\vec{S}_j \times \vec{S}_k)$ and are the manifestation of time-reversal symmetry breaking; these may be calculated within fourth-order perturbation theory [14,51]. The vanishing of chiral terms as N increases is shown in Fig. 2(b). These analytical results agree well with the exact numerical sums, for Ω detuned from the resonances and sufficiently large $N \gtrsim 10$. Moreover, they agree with the simple average of the monochromatic Floquet results over all linear polarizations.

In this concrete example, we can address the experimental feasibility of the timescales. The time for the spins to relax to the new low energy state given by the nonequilibrium exchange couplings is $T_{\rm rel} \sim 1/|J_1|$. The spins must feel the *unpolarized* exchange couplings, and so $T_{\rm rel} \gg T_p$. All this, and the measurement must happen within a single laser pulse. Most generously, we require $T_{\rm pulse} \gg T_{\rm rel} \gg T_p \gg T$, where $T_{\rm pulse}$ is the duration of the pulse. When this hierarchy of timescales is fulfilled, experiments should realize the effective models discussed here, not the time-dependent set of couplings $J_1^{(\delta_l)}(t)$. We further discuss the timescales in the Supplemental Material to argue that these are experimentally plausible [51].

Now we turn to general unpolarized light, where different protocols can lead to different physics. Any polarization profile can be decomposed into Stokes parameters [66],

$$\vec{S} = I(\cos 2\chi \cos 2\psi, \cos 2\chi \sin 2\psi, \sin 2\chi), \qquad (8)$$

which describe the surface of a sphere of radius $\sqrt{I}$: the Poincaré sphere (Fig. 1), where I is the intensity. For fixed monochromatic light, $\vec{S}$ describes a point on the surface. The poles, $\chi = \pm\pi/4$ correspond to left and right circularly polarized (CP) light, respectively, while linear polarization (LP) lies on the equator ($\chi = 0$), with angle ψ. For unpolarized, nearly monochromatic light, the polarization vector slowly traverses a periodic path on the Poincaré sphere with characteristic time $T_p = 2\pi/\Omega_p \gg T = 2\pi/\Omega$, such that the time average of the Stokes parameters is zero, $\langle\vec{S}\rangle = 0$ [28,66–73], of which the above case is one example. Generically, effective couplings in correlated systems are sensitive to the type of unpolarized light, which can be tuned. Unpolarized light is differentiated by higher-order correlators of the Stokes parameters $\langle S_i S_j\rangle$, $\langle S_i S_j S_k\rangle$, etc. [74], which must also preserve lattice and time-reversal symmetries for the correlated physics to respect those symmetries.

To preserve lattice and time-reversal symmetries, polarization distributions $f(\chi,\psi)$ must be invariant under rotations and have zero net chirality. Such distributions generate "type II" light [75]. We have already discussed type II Glauber light, which samples all LPs equally, encompassing the equator of the Poincaré sphere. Generic type II light may be constructed from superpositions of distributions with circles at $\chi = \pm\chi_0$, $f(\chi,\psi) = \frac{1}{2}[\delta(\chi-\chi_0) + \delta(\chi+\chi_0)]$. Type I light is more restrictive, sampling the Poincaré sphere uniformly, $f(\chi,\psi) = 1$ [75]. Fixed intensity type I light is known as amplitude-stabilized unpolarized light, while natural light has a varying intensity, $f(I,\chi,\psi) = (2/I_0)\exp(-2I/I_0)$ [76]; for exchange couplings, these give identical results after averaging over I. It is possible to generate nearly monochromatic type II Glauber [68] and type I light [67,69], either using spatial depolarizers or by superimposing slightly frequency detuned incoherent laser beams with orthogonal polarizations [51].

Any type of unpolarized light may be explicitly constructed by combining pairs of detuned lasers. The example above used a pair with equal weights of detuned left circularly polarized (LCP) and right circularly polarized (RCP) beams to produce a polarization vector traversing the equator. Any latitude may be traversed using a similar pair with unequal weights, and our analysis can proceed similarly. Different latitudes may then be superimposed by superimposing incoherent pairs of beams [77]. Therefore, for any type, we can calculate the couplings for an arbitrary fixed polarization for monochromatic light (see Supplemental Material [51]) and simply average over the polarization distribution [78], as shown in the previous example. For a given protocol, the magnetic exchange couplings J_{ij} are found by averaging

$$\langle J_{ij}\rangle = \frac{\int_{-\pi/4}^{\pi/4} d\chi \int_0^\pi d\psi \cos 2\chi f(\chi,\psi) J_{ij}(\chi,\psi)}{\int_{-\pi/4}^{\pi/4} d\chi \int_0^\pi d\psi \cos 2\chi f(\chi,\psi)}. \quad (9)$$

To demonstrate how varying the polarization protocol can drive materials through different regions of phase space, we explicitly consider the triangular lattice. It provides an apt example, as multiple spin liquids are accessible via different directions in phase space. While the nearest-neighbor (J_1) model has 120° order, spin liquids may be accessed by adding second neighbor (J_2), chiral (J_χ), or ring exchange ($J_\Box$) terms. There is a Dirac spin liquid for $J_2/J_1 \gtrsim 0.1$ [27–34], a chiral spin liquid for either $J_\chi/J_1 \gtrsim 0.2$ and $J_2 = 0$ or $J_\chi/J_1 \gtrsim 0.025$ for $J_2/J_1 \sim 0.1$ [32], and a spinon Fermi surface state for $J_\Box/J_1 \gtrsim 0.2$ [79]. The relevant Floquet engineered couplings may be found by expanding in $U + m\Omega$ either via the Brillouin-Wigner perturbation theory to fourth order [48,49], used in this Letter, or a Schrieffer-Wolff transformation [50] (details in the Supplemental Material [51]). Here, we fix the polarization and later average following Eq. (9) to find the desired unpolarized result.

To maximally enhance the further neighbor exchange couplings, we must approach the resonances at $\Omega = -U/m$. Yet, if the frequency is too close, doublons and holons are excited and heating is a serious problem. The Hubbard bands have a finite bandwidth $2\gamma t_1$, where γ is lattice dependent ($\gamma = 2\sqrt{5}$ for the triangular lattice [80]), so to avoid heating upon approaching the $U = \Omega$ resonance from below, we keep $\Omega < U - 2\gamma t_1$. [81] We also must insist, given our fluences, that *two* photons cannot excite electrons between Hubbard bands, $2\Omega > U + 2\gamma t_1$ [82]. This restriction limits potential materials, as only strongly insulating materials with $t_1 < U/(6\gamma)$ allow strong enhancements without heating. We fix $t_1 = U/(6\gamma)$ and $\Omega/U = 2/3$ to avoid heating while maximizing the enhancements; see the red vertical line in Fig. 2(a). Sufficiently far from resonance, there is minimal heating even for large fluences [14]. We calculated the enhancements of J_1, J_2, J_3, and $J_\Box$ for all kinds of type II and type I light. J_2/J_1 is maximally enhanced by either type I light, type II light with only equal parts LCP and RCP light, or *CP* light, which also generates J_χ. We show both the absolute change, Fig. 3(a), and enhancement over equilibrium values, Fig. 3(b), as functions of fluence. Because of the Bessel function structure, moderate fluences maximize the enhancement [83]. The absolute changes can be as large as 25% and 33% of the critical J_χ/J_1 and J_2/J_1, respectively. While these will not drive the t_1 Hubbard model into a spin liquid, a material with sufficiently large preexisting J_2, due either to second neighbor hopping or

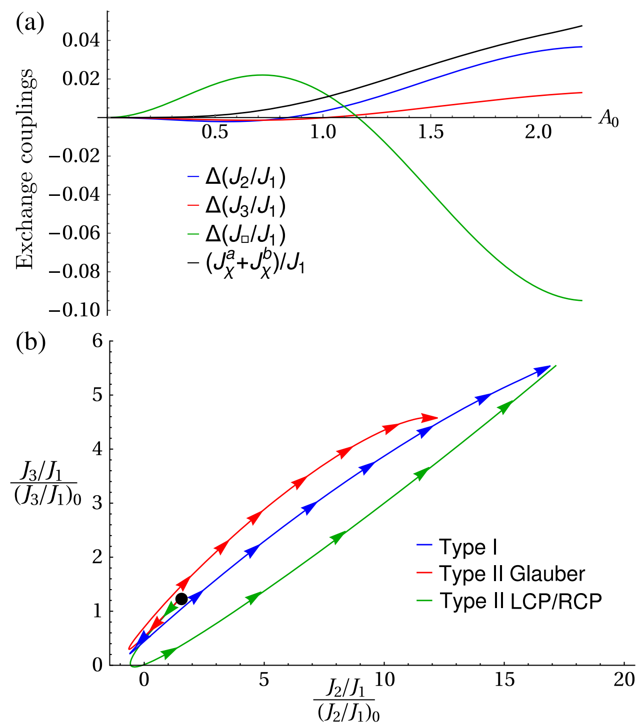

FIG. 3. Enhancement of magnetic couplings on the triangular lattice as functions of fluence. (a) Absolute changes for *CP* light with $\Omega = 2U/3$, where the enhancement is largest. J_2/J_1 and J_3/J_1 can be enhanced by 0.03 and 0.01, respectively. These may seem small, but are nearly 2000% and 500% of the equilibrium values, as shown in (b), and are a significant fraction of the J_2/J_1 required for the Dirac spin liquid. The effective chiral field reaches $\sim 0.05 J_1$ [51], again a significant fraction of the critical field. Ring exchange $J_\Box/J_1$ ranges between −0.09 and 0.02; positive values eventually induce a spin liquid but must be $10\times$ larger. (b) Different types of unpolarized light drive different paths through phase space, given in terms of the relative enhancement. A dot indicates the initial equilibrium point ($A_0 = 0$). Type I light (blue) samples the Poincaré sphere evenly, type II Glauber light (red) samples all linearly polarized light equally, and type II LCP/RCP (green) samples only the poles of the Poincaré sphere, eliminating chiral fields. Note that the *CP* light used in (a) gives identical results to type II LCP/RCP for J_1, J_2, and J_3.

superexchange, could be tuned to both Dirac and chiral spin liquids via different protocols. These absolute changes understate the enhancement, as the equilibrium values are tiny for the t_1/U required to avoid heating, and the enhancement of J_2/J_1 can be as large as 2000%.

Polarization protocols trace out unique paths through the J_2/J_1–J_3/J_1 phase space, as shown in Fig. 3(b), where J_3/J_2 varies by a factor of 2. Minimizing J_3 is essential to access the Dirac spin liquid, as J_3 increases the critical J_2 [34], and so type I or LCP and RCP averaged light is more favorable than type II Glauber. Note that we show two extremes of type II light ($\chi = 0, \pm\pi/4$), but all type II light lies between these.

We have shown that unpolarized light provides an untapped tuning parameter for Floquet engineering and possibly nonequilibrium physics, in general, particularly for correlated materials sensitive to higher-order correlations in the polarization. We showed that calculations can be done using Floquet techniques with fixed polarization and then averaged, as long as the polarization vector varies sufficiently slowly ($T_p \gtrsim 10T$). We illustrated this effect on magnetic exchange couplings for the triangular lattice and showed how different types of unpolarized light drive the model through varied directions in phase space. In particular, the same J_1–J_2 triangular material could be nudged into either Dirac or chiral spin liquids by different polarization protocols. Similar effects should be found throughout correlated materials. Future research might examine incommensurate frequencies, where the pseudorandom nature of the polarization variation may have interesting effects.

We acknowledge useful discussions with Thomas Iadecola, Eduardo Miranda, Peter Orth, Paraj Titum, Thais Trevisan, Chirag Vaswani, and Jigang Wang. V. L. Q and R. F. and were supported by NSF through Grant No. DMR-1555163. R. F. thanks the Aspen Center for Physics, supported by the NSF Grant No. PHY-1607611, for hospitality.

*vquito@iastate.edu

[1] T. Oka and S. Kitamura, Annu. Rev. Condens. Matter Phys. **10**, 387 (2019).
[2] J. H. Mentink, K. Balzer, and M. Eckstein, Nat. Commun. **6**, 6708 (2015).
[3] J. H. Mentink, J. Phys. Condens. Matter **29**, 453001 (2017).
[4] A. Ono and S. Ishihara, Phys. Rev. B **98**, 214408 (2018).
[5] J. M. Losada, A. Brataas, and A. Qaiumzadeh, Phys. Rev. B **100**, 060410(R) (2019).
[6] N. Walldorf, D. M. Kennes, J. Paaske, and A. J. Millis, Phys. Rev. B **100**, 121110(R) (2019).
[7] S. Chaudhary, D. Hsieh, and G. Refael, Phys. Rev. B **100**, 220403(R) (2019).
[8] M. M. S. Barbeau, M. Eckstein, M. I. Katsnelson, and J. H. Mentink, SciPost Phys. **6**, 27 (2019).
[9] F. Giustino *et al.*, J. Phys. Mater. **3**, 042006 (2021).
[10] M. S. Rudner and J. C. W. Song, Nat. Phys. **15**, 1017 (2019).
[11] M. Sato, Y. Sasaki, and T. Oka, arXiv:1404.2010.
[12] M. Sato, S. Takayoshi, and T. Oka, Phys. Rev. Lett. **117**, 147202 (2016).
[13] S. Kitamura, T. Oka, and H. Aoki, Phys. Rev. B **96**, 014406 (2017).
[14] M. Claassen, H.-C. Jiang, B. Moritz, and T. P. Devereaux, Nat. Commun. **8**, 1192 (2017).
[15] T. Oka and H. Aoki, Phys. Rev. B **79**, 081406(R) (2009).
[16] T. Kitagawa, T. Oka, A. Brataas, L. Fu, and E. Demler, Phys. Rev. B **84**, 235108 (2011).
[17] N. H. Lindner, G. Refael, and V. Galitski, Nat. Phys. **7**, 490 (2011).
[18] I. Martin, G. Refael, and B. Halperin, Phys. Rev. X **7**, 041008 (2017).
[19] Y. Baum and G. Refael, Phys. Rev. Lett. **120**, 106402 (2018).
[20] L. Yuan, Q. Lin, M. Xiao, and S. Fan, Optica **5**, 1396 (2018).
[21] T. Ozawa and H. M. Price, Nat. Rev. Phys. **1**, 349 (2019).
[22] A. Dutt, Q. Lin, L. Yuan, M. Minkov, M. Xiao, and S. Fan, Science **367**, 59 (2020).
[23] Y. H. Wang, H. Steinberg, P. Jarillo-Herrero, and N. Gedik, Science **342**, 453 (2013).
[24] J. W. McIver, B. Schulte, F.-U. Stein, T. Matsuyama, G. Jotzu, G. Meier, and A. Cavalleri, Nat. Phys. **16**, 38 (2020).
[25] L. Balents, Nature (London) **464**, 199 (2010).
[26] B. Mukherjee, Phys. Rev. B **98**, 235112 (2018).
[27] W.-J. Hu, S.-S. Gong, W. Zhu, and D. N. Sheng, Phys. Rev. B **92**, 140403(R) (2015).
[28] Z. Zhu and S. R. White, Phys. Rev. B **92**, 041105(R) (2015).
[29] P. H. Y. Li, R. F. Bishop, and C. E. Campbell, Phys. Rev. B **91**, 014426 (2015).
[30] Y. Iqbal, W.-J. Hu, R. Thomale, D. Poilblanc, and F. Becca, Phys. Rev. B **93**, 144411 (2016).
[31] S. N. Saadatmand and I. P. McCulloch, Phys. Rev. B **96**, 075117 (2017).
[32] A. Wietek and A. M. Läuchli, Phys. Rev. B **95**, 035141 (2017).
[33] S.-S. Gong, W. Zhu, J.-X. Zhu, D. N. Sheng, and K. Yang, Phys. Rev. B **96**, 075116 (2017).
[34] S.-S. Gong, W. Zheng, M. Lee, Y.-M. Lu, and D. N. Sheng, Phys. Rev. B **100**, 241111(R) (2019).
[35] L. Messio, C. Lhuillier, and G. Misguich, Phys. Rev. B **87**, 125127 (2013).
[36] W.-J. Hu, S.-S. Gong, and D. N. Sheng, Phys. Rev. B **94**, 075131 (2016).
[37] J. H. Shirley, Phys. Rev. **138**, B979 (1965).
[38] H. Sambe, Phys. Rev. A **7**, 2203 (1973).
[39] G. Mahan, *Condensed Matter in a Nutshell* (Princeton University Press, Princeton, NJ, 2010).
[40] T. Mikami, S. Kitamura, K. Yasuda, N. Tsuji, T. Oka, and H. Aoki, Phys. Rev. B **93**, 144307 (2016).
[41] J. Berges, S. Borsányi, and C. Wetterich, Phys. Rev. Lett. **93**, 142002 (2004).
[42] D. Abanin, W. De Roeck, W. W. Ho, and F. Huveneers, Commun. Math. Phys. **354**, 809 (2017).
[43] T. Mori, T. Kuwahara, and K. Saito, Phys. Rev. Lett. **116**, 120401 (2016).
[44] L. D'Alessio and M. Rigol, Phys. Rev. X **4**, 041048 (2014).

[45] A. Lazarides, A. Das, and R. Moessner, Phys. Rev. E **90**, 012110 (2014).

[46] T. Kuwahara, T. Mori, and K. Saito, Ann. Phys. (Amsterdam) **367**, 96 (2016).

[47] M. Abramowitz and I. Stegun, *Handbook of Mathematical Functions with Formulas, Graphs, and Mathematical Tables*, Applied Mathematics Series (U.S. Government Printing Office, Washington, DC, 1970).

[48] I. Lindgren, J. Phys. B **7**, 2441 (1974).

[49] P. Mohan, R. Saxena, A. Kundu, and S. Rao, Phys. Rev. B **94**, 235419 (2016).

[50] M. Bukov, M. Kolodrubetz, and A. Polkovnikov, Phys. Rev. Lett. **116**, 125301 (2016).

[51] See Supplemental Material at http://link.aps.org/supplemental/10.1103/PhysRevLett.126.177201 for a review of the monochromatic case, the perturbation theory structure, and discussion of time scales and experimental details, which includes [52–65].

[52] K. Hejazi, J. Liu, and L. Balents, Phys. Rev. B **99**, 205111 (2019).

[53] T. Li, A. Patz, L. Mouchliadis, J. Yan, T. A. Lograsso, I. E. Perakis, and J. Wang, Nature (London) **496**, 69 (2013).

[54] A. Sell, A. Leitenstorfer, and R. Huber, Opt. Lett. **33**, 2767 (2008).

[55] A. C. Potter, T. Senthil, and P. A. Lee, Phys. Rev. B **87**, 245106 (2013).

[56] D. V. Pilon, C. H. Lui, T. H. Han, D. Shrekenhamer, A. J. Frenzel, W. J. Padilla, Y. S. Lee, and N. Gedik, Phys. Rev. Lett. **111**, 127401 (2013).

[57] A. Pustogow, Y. Saito, E. Zhukova, B. Gorshunov, R. Kato, T.-H. Lee, S. Fratini, V. Dobrosavljević, and M. Dressel, Phys. Rev. Lett. **121**, 056402 (2018).

[58] J. R. Colbert, H. D. Drew, and P. A. Lee, Phys. Rev. B **90**, 121105(R) (2014).

[59] W. Burns, J. Lightwave Technol. **1**, 475 (1983).

[60] J. P. M. Jr. and R. A. Chipman, Opt. Eng. (Bellingham, Wash.) **29**, 1478 (1990).

[61] N. Hodgson and H. Weber, *Laser Resonators and Beam Propagation: Fundamentals, Advanced Concepts, Applications*, Springer Series in Optical Sciences (Springer, Berlin, Heidelberg, 2005).

[62] A. H. MacDonald, S. M. Girvin, and D. Yoshioka, Phys. Rev. B **37**, 9753 (1988).

[63] A. L. Chernyshev, D. Galanakis, P. Phillips, A. V. Rozhkov, and A. M. S. Tremblay, Phys. Rev. B **70**, 235111 (2004).

[64] V. L. Quito and R. Flint, arXiv:2003.05933.

[65] J. R. Schrieffer and P. A. Wolff, Phys. Rev. **149**, 491 (1966).

[66] M. Born and E. Wolf, *Principles of Optics: Electromagnetic Theory of Propagation, Interference and Diffraction of Light* (Elsevier Science, New York, 2013).

[67] G. Piquero, L. Monroy, M. Santarsiero, M. Alonzo, and J. C. G. de Sande, J. Opt. **20**, 065602 (2018).

[68] D. Colas, L. Dominici, S. Donati, A. A. Pervishko, T. C. Liew, I. A. Shelykh, D. Ballarini, M. de Giorgi, A. Bramati, G. Gigli, E. d. Valle, F. P. Laussy, A. V. Kavokin, and D. Sanvitto, Light Sci. Appl. **4**, e350 (2015).

[69] A. M. Beckley, T. G. Brown, and M. A. Alonso, Opt. Express **18**, 10777 (2010).

[70] N. Ortega-Quijano, J. Fade, F. Parnet, and M. Alouini, Opt. Lett. **42**, 2898 (2017).

[71] A. Shevchenko, M. Roussey, A. T. Friberg, and T. Setälä, Optica **4**, 64 (2017).

[72] A. Shevchenko and T. Setälä, Phys. Rev. A **100**, 023842 (2019).

[73] A. Hannonen, K. Saastamoinen, L.-P. Leppänen, M. Koivurova, A. Shevchenko, A. T. Friberg, and T. T. Setälä, New J. Phys. **21**, 083030 (2019).

[74] D. Klyshko, J. Exp. Theor. Phys. **84**, 1065 (1997).

[75] J. Lehner, U. Leonhardt, and H. Paul, Phys. Rev. A **53**, 2727 (1996).

[76] J. Goodman, *Statistical Optics*, Wiley Series in Pure and Applied Optics (Wiley, New York, 2015).

[77] Coherent superpositions will create more complicated Lissajous figures.

[78] We fix the intensity, but it may vary, as for natural light [66].

[79] O. I. Motrunich, Phys. Rev. B **72**, 045105 (2005).

[80] J. Liu, K. Hejazi, and L. Balents, Phys. Rev. Lett. **121**, 107201 (2018).

[81] Approaching from above ($\Omega > U + 2\gamma t_1$) does not lead to substantial enhancements.

[82] Fortunately, considering m photons does not lead to further restrictions.

[83] We must also take care to remain in the regime where perturbation theory makes sense, as the fourth-order corrections to J_1 can potentially drive it negative for some range of fluences. This is further discussed in the Supplementary Material [51].